International Geology Review, Vol. 48, 2006, p. 420–442.

Platinum-Group-Element Systematics of Peridotites from Ophiolite Complexes of Northwest Anatolia, Turkey: Implications for Mantle Metasomatism by Melt Percolation in a Supra-subduction Zone Environment

ERCAN ALDANMAZ[1] AND NECLA KOPRUBASI

Department of Geology, University of Kocaeli, Izmit 41040, Turkey

Abstract

Platinum-group-element (PGE) studies of peridotites from the supra-subduction zone (SSZ) ophiolites of northwest Anatolia provide evidence for the nature of melt extraction within the uppermost mantle, and interactions between subduction-related magma and oceanic lithosphere. The peridotite samples from the mantle section of the ophiolites are mainly spinel-harzburgites and dunites, accompanied by subordinate amounts of spinel-lherzolite. Whole-rock major-trace element and mineral chemical characteristics indicate that the peridotites originated as the solid residues of varying degrees of partial melting (~5 to ~20%), and were subsequently modified by interaction with metasomatizing melts. The samples have non-chondritic, fractionated chondrite-normalized PGE patterns. Melt-depleted (e.g., low Al_2O_3 and CaO contents) mantle harzburgites and dunites show moderate to strong enrichments in the palladium group relative to the iridium group PGEs (Pd_N/Ir_N = 1.81±0.23; N = CI-chondrite normalized), and in most samples, pronounced Rh and Pd enhancements relative to Pt (Rh_N/Pt_N = 2.31 ± 0.66; Pd_N/Pt_N = 1.93 ± 0.20). These signatures cannot be reconciled with a simple *in situ* melt extraction and removal of sulfide phases, but most likely reflect a multi-stage petrogenetic process that selectively enriched the local mantle environment in incompatible and less refractory siderophile elements that are mobilized during continuous melt percolation, while relatively depleting the mantle wedge in Pt, which was not as effectively mobilized by silicate melts (or fluids).

The results of quantitative model calculations indicate that the addition of sulfides that originated from interaction between solid mantle and percolating hydrous basaltic melts may account for the strongly supra-chondritic ratios of both Pd/Ir and Ir/Os, as well as for the formation of abundant chromite deposits within the ophiolite complex. The peridotites show no systematic variation of Ir-group PGE (Ir, Ru, Os; I-PGE) abundances relative to melt depletion indices such as Mg#, Al_2O_3, CaO, or spinel Cr#, despite their remarkable inter-element PGE variations. These along with elevated values of strongly incompatible lithophile elements (e.g., Ba, U, and LREE) in the reactive harzburgites and dunites suggest a post-melting metasomatism and melt impregnation in a supra-subduction zone environment. Enrichment in various incompatible elements (Hf, U, Ta, Sr) relative to the expected values for melt-depleted mantle residues and pronounced negative anomalies in fluid-insoluble high-field-strength elements (Ta, Nb, Zr, Hf, Ti) further suggest that both siliceous melts and slab-derived hydrous fluids were involved in mantle metasomatism.

Introduction

THE RELATIVE ABUNDANCES of platinum-group elements (PGEs) in mantle samples can be used to provide insights into a great variety of mantle processes, such as mantle melting, melt percolation, and mantle metasomatism (e.g., Morgan et al., 2001; Pattou et al., 1996). With their strongly siderophile character, PGEs are usually assessed to have been largely incorporated into the Earth's metallic core during core-mantle segregation. A large number of high-precision analyses of PGEs from various tectonic settings, however, have recently been interpreted as supporting the idea of a PGE excess in the upper mantle, which would record a heterogeneous distribution of these elements within the mantle (e.g., Rehkämper et al., 1997; Lorand and Allard, 2001). In this context, non-chondritic inter-element

[1]Corresponding author; email: ercan.aldanmaz@dunelm.org.uk

PGE fractionations and small to moderate deviations from chondritic abundances have been ascribed either to original variations in certain parts of the mantle (e.g. compositional heterogeneity related to a late meteoritic veneer; Morgan et al., 2001) or to core-mantle exchanges related to deep-seated thermal upwelling (e.g., mantle plumes originating from the core mantle boundary), possibly delivering additional siderophile elements from the core to the primitive upper mantle (e.g., Snow and Schmidt, 1998).

An alternative to these hypotheses is that such fractionations in PGEs are due to recent melt extraction (and infiltration) processes in the shallow (uppermost) mantle, and have no bearing on the heterogeneity and the processes occurring in the deep mantle. Osmium isotopic studies of relatively fertile peridotites, for instance, support the hypothesis of a primitive upper mantle characterized by chondritic evolution of Re/Os and Pt/Os (e.g., Brandon et al., 2000; Meisel et al., 1996, 2001). A large number of recent studies also provide evidence that the less refractory PGEs (Pd and Pt) fractionate during adiabatic partial melting (e.g., Lorand et al., 1999; Rehkämper et al., 1999; Puchtel and Humayun, 2001), leading to the view that intimate relationships between incompletely extracted partial melts and positive Pd (and Pt) anomalies in variably depleted mantle peridotites can most likely be interpreted to signify the effects of melt extraction on PGE relative abundances (e.g., Luguet et al., 2001, 2003).

The effects of melt metasomatism on PGE distributions of mantle residues, however, are not well constrained due mainly to the complicating effects of the variety of petrogenetic processes, including wide range of metasomatic agents (e.g., basaltic melts, volatile-rich alkaline melts, alkali-silica–rich melts), and variable melt/rock ratios (e.g., Lenoir et al., 2000). The variable effect of melt/rock reactions on PGE behavior has been documented in a number of recent attempts; some bulk-rock studies did not detect significant effects (e.g., Handler and Bennett, 1999), whereas others have identified coupled enrichment of Pt, Pd, Cu, and S resulting from precipitation of PGE-rich sulfides of metasomatic origin (Alard et al., 2000; Lorand and Allard, 2001; Griffin et al., 2002). Some recent studies also provided evidence that percolation of basaltic melts at high melt/rock ratios can change the PGE relative abundances of mantle rocks significantly, by removing the sulfide phases residual from previous melting events and resulting in sulfides re-equilibrated with the percolating melts in terms of their PGE budgets (e.g. Büchl et al., 2002; Lorand et al., 2003). One should therefore expect that the fractionated patterns of PGEs provide important information regarding the history of mantle rocks, and precise determination of the relative abundances of highly siderophile elements may shed light on processes that have obscured the original signature of upper-mantle rocks.

The Northwest Anatolian orogenic complex contains a number of ophiolite fragments that are considered to represent remnants of oceanic lithosphere formed in supra-subduction zone (SSZ) tectonic settings (Okay et al., 1998; Önen, 2003; Beccaletto and Jenny, 2004). The rocks of these mantle representatives were emplaced mostly onto passive-margin sequences of the Anatolite-Tauride platform as a result of the Mesozoic accretion of continental blocks (or arc-related terranes). This suite of ophiolites provides the opportunity to examine inter-element PGE fractionation during relatively large degrees of melting and subduction-induced mantle metasomatism, because textural and chemical characteristics of the rocks indicate that they experienced melt extraction and extensive melt/rock interaction. The large, reactive dunite and harzburgite lenses within the mantle section of the ophiolites contain abundant chromite deposits, the formation of which can most likely be explained within the general context of melt/rock or melt/melt interaction during melt percolation (e.g., Zhou et al., 1996, 1998; Melcher et al., 1997; Ballhaus, 1998).

In this contribution, we combine whole-rock lithophile-, calcophile- and siderophile-element systematics of the residual mantle rocks sampled from Northwest Anatolian ophiolites, with a special emphasis on ascertaining mechanisms controlling PGE distributions and the influence of percolating fluids (or melts) on the behavior of PGEs and Cr in the Earth's upper mantle. We also evaluate the relative importance of partial melting, melt/rock interaction and mantle compositional evolution in the supra-subduction zone mantle of northwest Anatolia.

Geological Background

The Northwest Anatolian ophiolite complex represents remnants of oceanic lithosphere interpreted to have formed in a supra-subduction zone tectonic setting, that floored a part of the northern Neo-tethys ocean (Sengor and Yilmaz, 1981) and, subsequent to

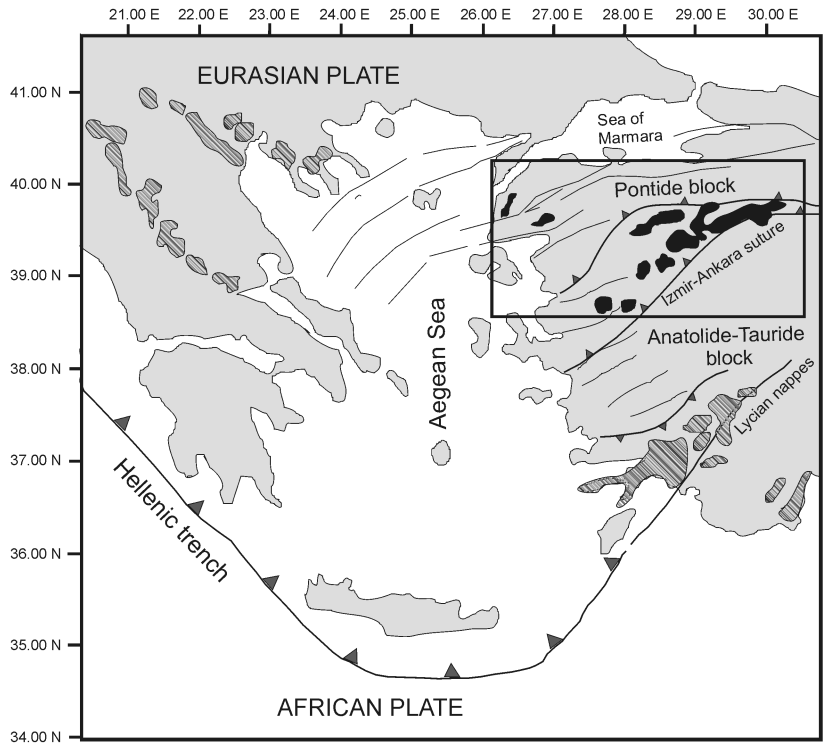

FIG. 1. Regional tectonic map showing the distribution of the Northwest Anatolian ophiolites (dark areas) and the other ophiolite bodies of the eastern Mediterranean (shaded areas).

Late Cretaceous (90 Ma; Okay et al., 1998; Önen, 2003) north-dipping subduction and plate collision, was emplaced onto passive-margin volcano-sedimentary sequences of Tauride-Anatolide platform. The ophiolites consist of a number of disrupted ultramafic bodies exposed along the northern Neo-Tethyan suture zone (Fig. 1). The original internal structure of the ophiolites was largely disrupted during emplacement. The rock types are predominantly harzburgite and dunite with minor lherzolite, gabbro, pyroxenite, and chromitite. Subvertical peridotite (mainly harzburgite and dunite) sheets with several kilometers of total thickness contain thin layers of gabro and pyroxenite. The peridotites show remarkable tectonic foliation that forms mainly parallel to the compositional layering and is defined by preferred orientation of olivine grains and elongate enstatite crystals (Okay et al., 1998). Thin pyroxenite layers within the peridotites are interpreted to represent crystal cumulates from mantle-derived magmas intruded as dikes and later were rotated toward subhorizontal foliation planes.

The rocks of the Northwest Anatolian ophiolites differ from "MORB"-type ophiolites in their mantle sequences, the more common presence of podiform chromite deposits, the existence of large proportions of reactive harzburgite and dunite bodies, and the crystallization of pyroxene before plagioclase, which is evident from the high abundances of pyroxenite relative to troctolite in the cumulate sequences. Volcanic arc–related geochemical signatures in the melt products of the ophiolites (e.g., gabbros and gabbroic dikes with high ratios of LILE/HFSE; Önen, 2003) may further imply that these ophiolites are fragments of oceanic lithosphere formed above a subduction zone. The general characteristics of the Northwest Anatolian ophiolites resemble those of many other classic examples of Mesozoic ophiolites of the eastern Mediterranean, Oman, and California, which are described as representing forearcs that formed during episodes of subduction initiation (e.g. Shervais, 2001).

In some parts of the Northwest Anatolian ophiolites, abundant chromite deposits are accompanied

by large elongated dunite lenses hosted in basal units of harzburgites within mantle sequences. Contacts between the dunite lenses and their host peridotites are relatively sharp, but the dunite envelopes around the chromite ore bodies grade outward into harzburgite. These sections are interpreted to mark zones of extensive melt-solid interaction, along which extensive chromite deposits form in a mode of either disseminated grains or rare massive chromitite layers.

Sample Description

The peridotites sampled from the Northwest Anatolian complex are moderately serpentinized (~20–40%, estimated by loss on ignition values; Table 1) mantle representatives. The rocks are predominantly harzburgites and dunites (with subordinate lherzolites) with original compositions of ~65–92% olivine, 5–20% orthopyroxene, 2–10% clinopyroxene, and accessory chrome spinel and chromite.

The lherzolites are composed dominantly of olivine and lesser amounts of orthopyroxene, clinopyroxene, and minor spinel. Most olivines have a grain size of up to 3 mm in diameter and show a meshwork texture where partly altered to serpentine. Orthopyroxenes are typically the largest minerals in the lherzolites, attaining diameters up to 5 mm. Clinopyroxene is variable in size, but not larger than 2 mm in diameter, with strongly concave boundaries and surrounded by fine-grained olivine. Spinels are generally fine grained and less than 2 mm in diameter.

Most of the harzburgites and dunites are essentially homogeneous, largely comprising olivine, orthopyroxene, and spinel, and resemble mantle restites (e.g., Bonatti and Michael, 1989). Olivine forms anhedral grains, 1–4 mm, many of which typically have kink-band textures. Orthopyroxene forms subhedral, generally tabular grains up to 10 mm long. Accessory chromite is anhedral in harzburgites but typically euhedral in dunites. The samples display typical coarse-granular textures characterized by a network of rounded orthopyroxene crystals immersed in an olivine matrix that may contain relict Cr-spinel. Most of the orthopyroxene grains have lobate boundaries, which may be interpreted as resulting from either incongruent dissolution of orthopyroxene or trapping during asthenospheric recrystallization. The reactive dunite samples display an abundant mesh texture of serpentine with relicts of olivine and disseminated chromite. Other non-silicate minerals associated with the chromite-rich harzburgites and dunites include magnetite, pyrite, pyrrhotite, millerite, ilmenite, chalcopyrite, and the PGE-bearing sulfide minerals valleriite, mackinawite, and pentdlandite.

Ultramafic cumulates consist of pyroxenite (websterite) and wehrlite. Some orthopyroxene grains in websterite are extremely coarse (up to 2 cm). Fine-grained clinopyroxene, orthopyroxene, and spinel generally surround them. Websterite contains orthopyroxene (60–65%), clinopyroxene (25–30%), olivine (0–5%), and spinel (1–3%), whereas wehrlite contains olivine (70–75%), clinopyroxene (5–25%), orthopyroxene (0–5%), and spinel (2–4%).

Bulk-Rock Chemistry

Whole-rock major-oxide and trace-element abundances for the peridotites were measured at the ALS Chemex Analytical Laboratories at Toronto. In order to obtain representative major- and trace-element analyses of coarse-grained peridotites, all rock powders were prepared from at least 2 kg of material and crushed to <125 μm in an agate ball mill. Rock powders were first fused to ensure dissolution of all phases and then dissolved in hot HF and HNO_3 to prepare the solutions from which major- and trace-element abundances were determined using ICP-AES and ICP-MS respectively. Loss on ignition (LOI) was determined by heating a separate aliquot of rock powder. Serpentine alteration, as reflected by the range of LOI, was corrected for by recalculating the whole-rock analyses as anhydrous compositions. Whole-rock major- and trace-element data for the mantle peridotites along with two samples of layered cumulate pyroxenite are given in Table 1.

PGE and Au concentrations of 13 ultramafic peridotites and two pyroxenites are presented in Table 2. PGE and Au analyses are by nickel sulfide fire assay–induced coupled plasma–mass spectrometry method at the same laboratory. NiS fire assay was done to pre-concentrate PGEs. The NiS button was dissolved in HCl and PGE phases were collected on a filter paper. Further dissolution of PGE phases was done following the procedures described in Plessen and Erzinger (1998). Analyses of spinels and olivines from the peridotites were performed using a Cameca CAMEBAX electron microprobe at the Blaise Pascal University (France), with operating conditions of 15 kV accelerating

TABLE 1. Whole-Rock Major Oxide and Trace-Element Data for Peridotites from Northwest Anatolian Ophiolites

Sample name:	NWA14	NWA9	NWA11	NWA19	NWA6	NWA18	NWA15	NWA17	NWA20	NWA8	NWA21	NWA12	NWA22	NWA29	NWA10
Rock type:	Lhz.	Lhz.	Lhz.	Hzb.	Hzb.	Hzb.	Hzb.	Du.	Hzb.	Du.	Hzb.	Du.	Du.	Px.	Px.
							wt%:								
SiO_2	43.44	43.07	44.20	42.62	42.34	42.37	42.88	42.22	42.44	41.42	42.06	40.44	42.63	49.77	48.81
TiO_2	0.03	0.02	0.03	0.02	0.02	0.02	0.02	0.01	0.03	0.02	0.02	0.01	0.02	0.07	0.06
Al_2O_3	3.10	2.79	3.37	2.46	2.42	2.34	2.28	1.69	2.09	1.59	2.18	0.98	2.15	1.52	1.30
FeO	8.29	8.52	8.55	8.88	8.90	8.90	8.56	8.47	8.01	9.48	8.90	8.92	8.82	5.54	5.94
MnO	0.11	0.11	0.11	0.12	0.11	0.13	0.11	0.10	0.10	0.13	0.12	0.11	0.12	0.11	0.12
MgO	42.30	42.50	40.10	43.30	43.70	43.30	43.80	45.30	43.80	46.10	44.10	47.90	44.20	23.10	25.30
CaO	2.25	2.85	3.01	1.92	1.81	2.41	1.87	0.95	1.56	0.93	1.82	0.42	1.51	18.25	16.70
Na_2O	0.05	0.04	0.13	0.03	0.02	0.02	0.04	0.02	0.04	0.01	0.03	0.01	0.02	0.10	0.09
K_2O	0.01	0.01	0.02	0.01	0.01	0.01	0.01	0.01	0.01	0.01	0.01	0.01	0.01	0.01	0.01
P_2O_3	0.01	0.01	0.01	0.01	0.01	0.01	0.01	0.01	0.01	0.01	0.01	0.01	0.01	0.01	0.01
LOI	7.46	8.12	13.20	8.61	7.83	8.26	8.27	9.81	8.95	8.14	8.46	8.69	10.05	0.84	1.37
Total (LOI free)	99.59	99.92	99.53	99.37	99.34	99.51	99.58	98.78	98.09	99.70	99.25	98.81	99.49	98.48	98.34
							ppm								
Ni	2145.8	2413.7	2417.2	2903.6	2556.4	2212.9	2384.2	2461.7	2413.6	2726.9	2468.6	2578.7	2782.8	1015.4	1741.6
Cr	3291	3306	3479	3444	2909	4291	3977	4332	3531	2977	3861	2655	4137	3339	2550
Rb	0.17	0.14	0.20	0.21	0.17	0.17	0.17	0.14	0.17	0.19	0.19	0.21	0.54	0.14	0.16
Sr	9.39	5.40	29.63	4.09	6.10	6.43	5.10	4.11	16.48	7.41	10.41	4.12	6.82	8.89	3.28
Y	2.74	2.41	2.43	0.66	1.93	3.02	0.88	0.66	0.85	0.46	0.55	0.49	0.71	2.75	2.12
Zr	3.03	2.13	5.65	2.03	3.43	2.33	3.21	2.52	3.30	4.85	3.20	1.76	2.19	4.85	2.13
Nb	0.18	0.14	0.32	0.12	0.12	0.13	0.11	0.11	0.30	0.20	0.19	0.16	0.23	0.14	0.10
Ba	3.51	2.62	3.63	3.64	2.76	4.37	3.78	2.75	4.71	4.23	3.47	2.84	5.37	2.88	2.89
La	0.32	0.14	1.32	0.26	0.16	0.18	0.22	0.13	0.66	0.35	0.72	0.27	0.30	0.19	0.12
Ce	0.85	0.39	3.25	0.55	0.46	0.49	0.48	0.32	1.60	0.86	1.37	0.49	0.61	0.65	0.38
Pr	0.13	0.07	0.42	0.07	0.07	0.08	0.07	0.05	0.21	0.11	0.15	0.06	0.09	0.11	0.07
Nd	0.68	0.39	1.72	0.24	0.40	0.43	0.32	0.25	0.90	0.44	0.53	0.25	0.40	0.61	0.41
Sm	0.21	0.14	0.35	0.06	0.14	0.17	0.09	0.07	0.18	0.08	0.08	0.05	0.09	0.22	0.14
Eu	0.08	0.06	0.11	0.02	0.06	0.08	0.03	0.02	0.05	0.03	0.02	0.02	0.03	0.09	0.06
Gd	0.28	0.22	0.33	0.08	0.21	0.29	0.10	0.08	0.15	0.07	0.07	0.06	0.09	0.31	0.24
Tb	0.06	0.05	0.06	0.02	0.04	0.06	0.02	0.02	0.03	0.01	0.01	0.01	0.02	0.06	0.05
Dy	0.39	0.34	0.36	0.10	0.27	0.46	0.13	0.10	0.14	0.08	0.08	0.07	0.11	0.41	0.32
Ho	0.10	0.08	0.08	0.02	0.07	0.11	0.03	0.02	0.03	0.02	0.02	0.02	0.03	0.10	0.08
Er	0.29	0.25	0.23	0.07	0.20	0.35	0.08	0.07	0.07	0.05	0.06	0.05	0.08	0.29	0.23
Tm	0.05	0.04	0.04	0.01	0.03	0.05	0.01	0.01	0.01	0.01	0.01	0.01	0.01	0.05	0.04
Yb	0.31	0.27	0.26	0.09	0.23	0.37	0.08	0.07	0.08	0.06	0.08	0.06	0.09	0.31	0.24
Lu	0.05	0.05	0.05	0.02	0.04	0.06	0.02	0.01	0.02	0.01	0.02	0.01	0.02	0.05	0.04
Hf	0.11	0.09	0.15	0.09	0.09	0.13	0.10	0.08	0.08	0.10	0.06	0.05	0.06	0.16	0.11
Ta	0.03	0.02	0.04	0.01	0.01	0.01	0.01	0.01	0.01	0.01	0.05	0.01	0.01	0.01	0.01
Th	0.03	0.02	0.05	0.05	0.04	0.07	0.05	0.04	0.05	0.07	0.05	0.10	0.06	0.02	0.02
U	0.02	0.01	0.03	0.01	0.02	0.02	0.01	0.01	0.02	0.02	0.03	0.03	0.04	0.01	0.01
$Mg\#_{WR}$	0.901	0.899	0.893	0.897	0.897	0.897	0.901	0.905	0.907	0.897	0.898	0.905	0.899		
$Mg\#_{ol}$	0.899	0.897	0.895	0.900	0.901	0.903	0.902	0.912	0.907	0.912	0.905	0.920	0.910		
$Cr\#_{sp}$	0.18	0.19	0.17	0.29	0.33	0.32	0.37	0.59	0.38	0.57	0.52	0.69	0.43		
$Mg\#_{sp}$	0.72	0.71	0.70	0.69	0.65	0.66	0.59	0.47	0.57	0.46	0.51	0.42	0.55		
F (%)[1]	6.85	7.39	6.28	11.62	12.91	12.61	14.06	18.72	14.32	18.38	17.46	20.29	15.56		

[1]The degree of partial melting F (in percent) as a function of spinel Cr# is expressed as [F = 10 ln(Cr#) + 24] following the calibration of Hellebrand et al. (2001) for spinel Cr# values between 0.17 to 0.69. Key to abbreviations: WR = whole-rock; ol = olivine; sp = spinel. Rock types are: lherzolite (Lhz), harzburgite (Hzb), pyroxenite (Px), and (Du) dunite.

TABLE 2. Chalcophile and Highly Siderophile Trace-Element Data for Peridotites from Northwest Anatolian Ophiolites[1]

Sample name:	NWA14	NWA9	NWA11	NWA19	NWA6	NWA18	NWA15	NWA17	NWA20	NWA8	NWA21	NWA12	NWA22	NWA29	NWA10
S, ppm	161.8	134.1	143.9	126.3	157.3	113.8	172.5	136.4	155.1	163.7	182.6	177.2	178.4	94.30	138.90
Cu, ppm	28.6	18.6	23.2	21.6	24.5	16.4	34.8	20.7	34.1	30.1	58.4	38.3	52.9	38.40	20.90
Os, ppb	4.83	4.11	3.24	4.43	3.17	3.27	3.26	3.81	2.85	2.69	4.17	1.45	2.57	1.93	1.52
Ir, ppb	4.75	4.37	3.52	3.72	4.64	3.92	4.65	3.42	3.27	3.61	4.36	2.67	3.62	1.02	2.28
Ru, ppb	6.53	6.15	5.46	6.28	7.28	6.36	6.27	5.17	4.61	5.72	7.06	3.35	4.34	1.14	2.95
Pt, ppb	10.56	8.27	7.36	7.56	9.17	8.73	11.32	8.11	8.36	6.11	9.33	3.53	8.61	16.58	5.84
Rh, ppb	2.21	2.07	1.82	2.30	2.18	2.11	2.73	2.52	2.47	2.81	2.75	1.74	2.54	2.95	2.28
Pd, ppb	9.35	8.14	8.71	8.24	8.92	10.16	10.64	8.05	8.19	7.52	9.69	4.32	8.84	6.93	5.62
Au, ppb	1.73	1.04	1.27	2.03	2.16	1.63	1.94	1.35	1.93	1.25	2.94	2.94	2.06	1.05	3.56
$(Os/Ir)_N$	0.94	0.87	0.85	1.11	0.63	0.77	0.65	1.03	0.81	0.69	0.89	0.50	0.66	1.76	0.62
$(Ru/Ir)_N$	0.88	0.90	0.99	1.08	1.01	1.04	0.86	0.97	0.90	1.02	1.04	0.80	0.77	0.72	0.83
$(Pt/Ir)_N$	1.00	0.85	0.94	0.92	0.89	1.00	1.10	1.07	1.15	0.76	0.96	0.60	1.07	7.32	1.15
$(Rh/Ir)_N$	1.63	1.66	1.81	2.16	1.64	1.88	2.05	2.58	2.64	2.72	2.21	2.28	2.46	10.12	3.50
$(Pd/Ir)_N$	1.63	1.54	2.05	1.83	1.59	2.14	1.89	1.95	2.07	1.72	1.84	1.34	2.02	5.62	2.04
$(Rh/Pt)_N$	1.63	1.94	1.92	2.36	1.85	1.88	1.87	2.41	2.30	3.57	2.29	3.83	2.29	1.38	3.03
$(Pd/Pt)_N$	1.63	1.81	2.17	2.00	1.79	2.14	1.73	1.82	1.80	2.26	1.91	2.25	1.89	0.77	1.77

[1]Chalcophile elements were analyzed by ICP-MS and highly siderophile elements are by nickel sulfide fire assay-induced ICP-MS.

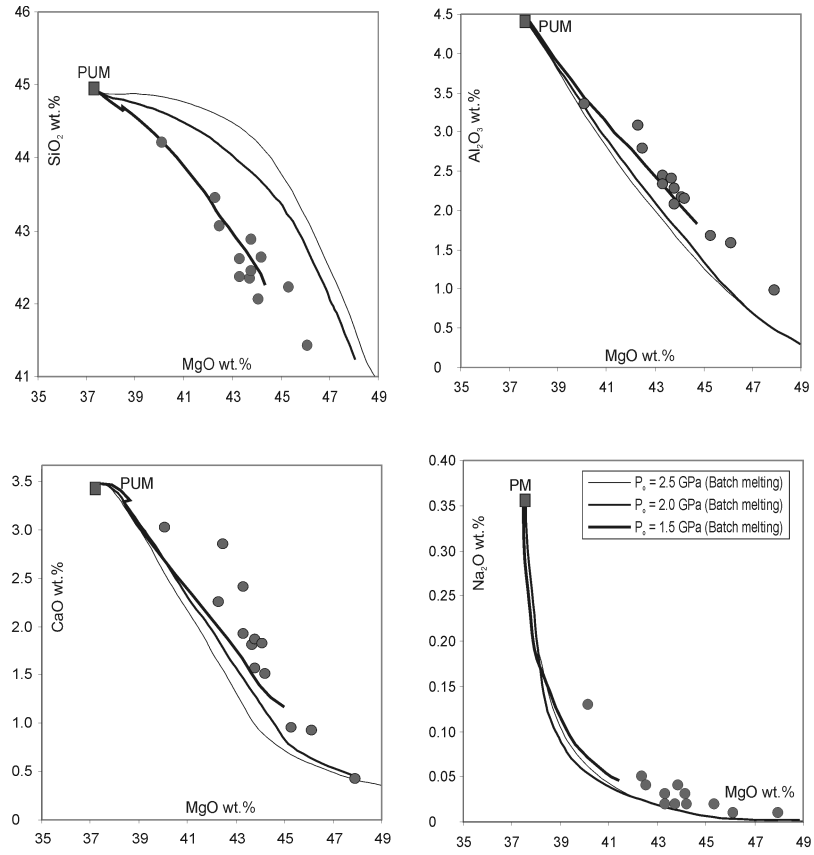

FIG. 2. Variations of whole-rock SiO_2, Al_2O_3, CaO, and Na_2O concentrations as a function of MgO in peridotites from Northwest Anatolian ophiolites. The curves represent the residues of incrementally isentropic polybaric batch melting calculated using the MELTS thermodynamic approach (Ghiorso and Sack, 1995). Calculations use the primitive upper mantle (PUM) composition of McDonough and Sun (1995) as a starting source. The curves correspond to melting pressures of 1.5, 2.0, and 2.5 GPa as indicated in the figure. The major-element variations are consistent with the calculated trends of experimental results for low-pressure (<1.5 GPa) partial melting of spinel-lherzolites.

voltage, 10–12 nA beam current, and 10 s counting time per element.

Major, minor, and transition elements

The variations in some whole-rock major-element concentrations for the 13 best-preserved spinel-peridotites from the Northwest Anatolian ophiolites are shown in Figure 2. Alteration, particularly serpentinization, can potentially be considered to have caused large changes to bulk chemistry, e.g. in Fe, Mg, Ca, Na, and K (Seyfried and Dibble, 1980). As a measure of the integrity of the chemical systems, the alkalis might be expected to increase during hydration. However, Na_2O and K_2O are both extremely low in abundances in all samples, suggesting that hydration processes, although creating some scatter in the trends, did not significantly affect the overall chemistry. Furthermore, the major-element abundances do not show any correlation with loss on ignition, indicating little or no sensitivity to alteration. Thus, any geochemical trends between samples are candidates for original features rather than reflecting variable degrees of alteration.

The peridotites overall display a remarkably variable degree of fertility with a range of MgO from 40 to 47 wt%. The MgO contents increase systematically from lherzolite to harzburgite to dunite and can be considered as an index of "melt depletion" (e.g., Parkinson and Pearce, 1998). Although some samples have fertile average major-element compo-

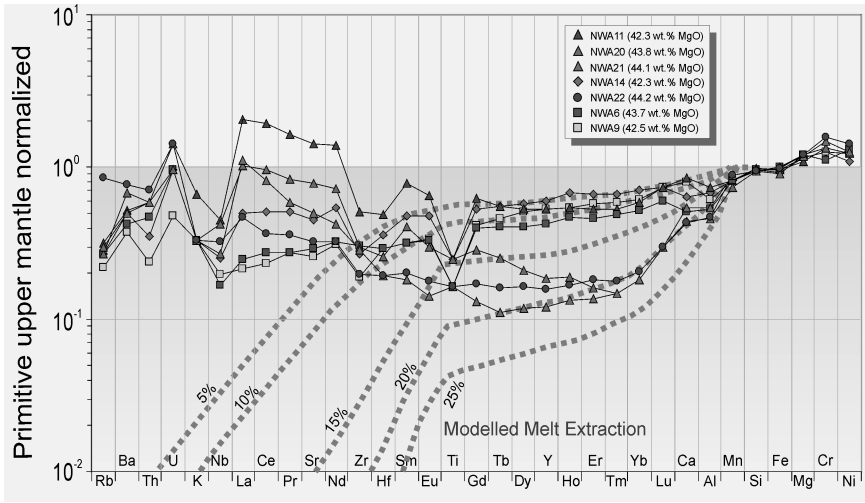

FIG. 3. Whole-rock multi-element abundances of peridotites from the Northwest Anatolian ophiolites represented on a primitive upper mantle (PUM)–normalized diagram. Dashed curves in the diagram illustrate the effect of dynamic extraction of different amounts of melt (5% to 25% melting within the spinel stability field, with mode and melt mode described in Kinzler, 1997) from a PUM composition. The modeling uses the mineral/matrix partition coefficients of McKenzie and O'Nions (1991) and the parameters described in Zou (1998). Normalizing values are from McDonough and Sun (1995).

sitions (i.e., rich in basaltic components with CaO ~3 %, Al_2O_3 >2.5 %, MgO <43 %) the majority of the peridotites are moderately to highly depleted in basaltic components and are more refractory than fertile upper-mantle composition (Table 1; Fig. 2). Whole-rock analyses indicate that the peridotites display a progressive trend of depletion in fusible elements such as Ca, Al, and Na with increasing the MgO content of the rocks. This depletion trend, which is accompanied by a decrease of the modal abundances of clinopyroxene and increase of those of olivine, is, to a first order, consistent with the formation of the peridotites as mantle residues from a variable extent of basaltic melt extraction (Fig. 2). The samples are mostly characterized by near-constant CaO/Al_2O_3 ratios consistent with continuous melt extraction from a source, but higher CaO/Al_2O_3 ratios (>0.8) in a number of samples may be considered indicative of calcium-rich melt metasomatism.

The chemical compositions of peridotite minerals can be used estimating the degree of melt extraction. We use an approach based on the numerical expression by Hellebrand et al. (2001). This parameter is based on the spinel Cr# [Cr/(Cr+Al)] (e.g., with increasing degree of partial melting, decreasing activity of aluminum in peridotite leads to an increase in equilibrium Cr# in spinel). The Cr# of the spinels from the studied peridotites range widely from 0.17 to 0.69 (Table 1) and lie predominantly within the range of ophiolites worldwide (e.g., Melcher et al., 1997). Results indicate that the studied peridotites are likely to be the residual products formed after 6.3 (±0.7) to 20.3 (±2.6)% basaltic melt extraction from a mantle source that is similar in composition to the primitive upper mantle (Table 1).

Incompatible trace elements

Primitive upper mantle (PUM)–normalized trace-element patterns for the peridotites are shown in Figure 3. The samples as a whole have incompatible trace-element concentrations that are generally lower than those of primitive mantle. In the majority of the samples, Sr and Y form smooth patterns with the REE, but negative Nb, Zr, Hf (and Ti for some samples) troughs are present. The peridotites display significantly greater concentrations of LREE and highly incompatible elements (in particular the fluid-soluble elements—K, U, and Ba) than expected for mantle residues, despite their variable degree of depletion in fusible major-element concentrations. This may suggest subsequent enrichment processes in the mantle melting region.

Chondrite-normalized whole-rock REE patterns for the Northwest Anatolian peridotites are shown in

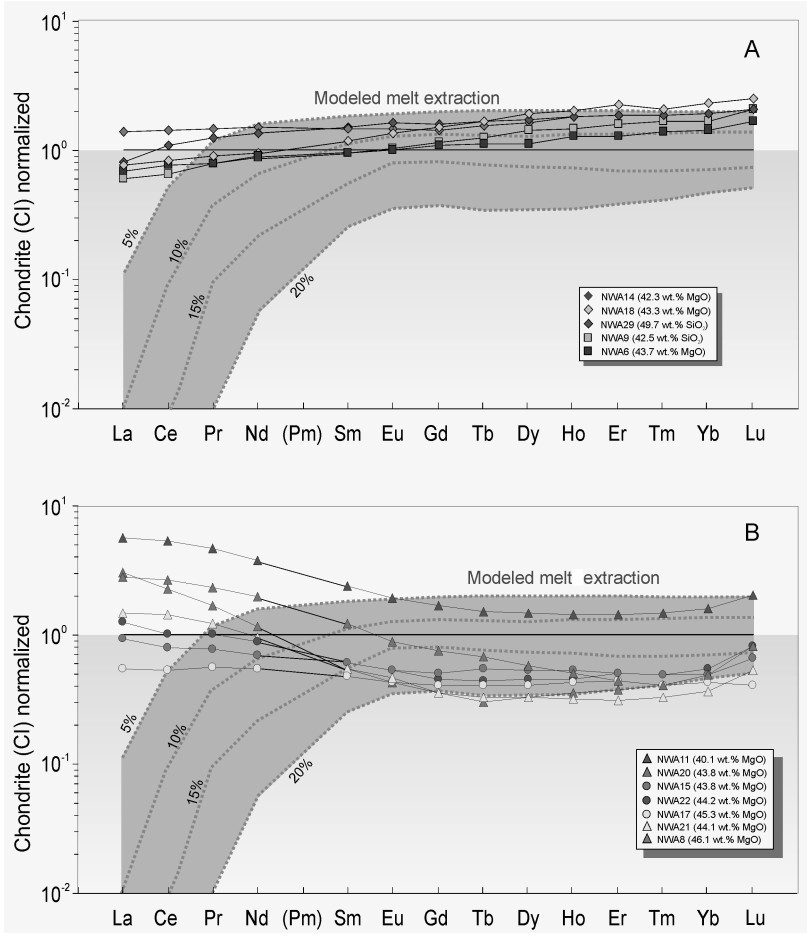

FIG. 4. Chondrite-normalized REE patterns for (A) melt-depleted and (B) refertilized peridotites from Northwest Anatolian ophiolites. Also plotted for comparison (the shaded field) is the range of model residual mantle compositions calculated using the approach described in Figure 3. The calculations assume 5% to 20% melt segregation from a PUM composition within the spinel stability field. Normalizing values and PUM compositions are from Anders and Grevesse (1989) and McDonough and Sun (1995), respectively.

Figure 4. The samples have low total REE contents, with LREE abundances of between 5.6 and 0.5 × CI chondrite, whereas HREE abundances are less variable, ranging between 2.0 and 0.4 × CI chondrite. Consistent with the interpretation from the major-element data, none of the samples show the highly modified, strongly LREE-depleted patterns that might be expected if serpentinization had affected the original chemistry significantly. Theoretically, in the upper mantle melting regimes, REEs behave incompatibly with spinel-bearing mantle residues, with the LREE being the most incompatible, which results in unmodified residua having LREE-depleted patterns. The lherzolite samples are characterized by a slight LREE depletion (La_N/Yb_N = 0.49–0.71; the subscript N denotes chondrite-normalized) with a flat to slightly fractionated HREE segments (Dy_N/Yb_N = 0.84–0.91; Fig. 4A). LREE profiles for the harzburgites and dunites, however, vary from slightly depleted to highly enriched (La_N/Yb_N = 0.48 and 6.23), consistent with some trapping of, or interaction with, melts or aqueous fluids containing high concentrations of highly incompatible LREE. Some samples show slightly concave

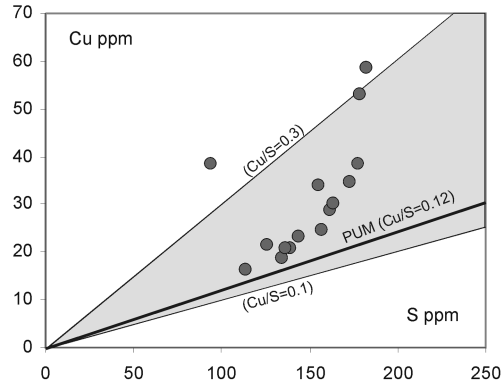

FIG. 5. Copper vs. sulfur plot for peridotites from the Northwest Anatolian ophiolites, illustrating their division on the basis of their Cu/S ratios. The heavy line denotes the primitive upper mantle Cu/S ratio of 0.12 (McDonough and Sun, 1995).

patterns with unfractionated HREE segments, and have U-shaped REE profiles owing to pronounced MREE depletions relative to HREE (Dy_N/Yb_N = 0.74 to 0.88; Fig. 4B). Similar characteristics are usually interpreted as resulting from interaction between an LREE-enriched melt and an LREE-depleted mantle residue (e.g., Pearce et al., 1999).

Overall, the incompatible trace-element patterns are consistent with a multi-stage evolution of the peridotites, indicating that the peridotites have experienced re-enrichment in LREE and other highly incompatible lithophile elements, in particular the fluid mobile elements K, U (e.g. relative to Th), and Ba. This suggests that the peridotites were metasomatized by hydrous fluids (or fluid-enriched melts) subsequent to the earlier melt extraction.

Chalcophile and siderophile elements

Sulfur abundances of peridotites range from 94 ppm to 186 ppm, and show no systematic correlation with the melt depletion indices of major oxides (e.g., MgO, Al_2O_3, or CaO). There is also no systematic variation of S with absolute PGE abundances, implying that the variation in S is unlikely to have been controlled solely by melt extraction. Similar characteristics of non-systematic variations between S and melt-depletion indices are observed in many other peridotite massifs worldwide and are usually interpreted as resulting from combination of mantle metasomatism and interaction with mantle melts (or fluids) rather than progressive loss of the mantle sulfides by increasing degree of partial melting. Figure 5 shows an apparent positive correlation between S and Cu abundances of the peridotites. The rocks as a whole plot in an area defined by Cu-S trends corresponding to Cu/S ratios of 0.12 and 0.30, and have Cu/S ratios greater than the estimated value for the silicate Earth (McDonough and Sun, 1995). Elevated values in Cu/S ratios relative to the average primitive upper mantle composition can be interpreted as reflecting precipitation of Cu-rich interstitial sulfides from basaltic melts that percolated through peridotite channels (e.g. Lorand et al., 1999; Alard et al., 2000).

Measured concentrations of whole-rock PGE and Au for the mantle rocks from Northwest Anatolia are listed in Table 2. Despite large variations in absolute PGE abundances, relative PGE abundances for individual samples do not vary significantly throughout the entire suite, indicating no significant within-suite variations. One of the pyroxenite samples analyzed, however, displays a PGE pattern that is characterized by extremely high Pd/Ir and Pt/Ir ratios. Such a pattern differs markedly from those of the other mantle peridotites from the same suite and is interpreted to have resulted from equilibration of significant amounts of the primary sulfide (rich in Pt and Pd) with mantle melt (probably associated with processes of melt percolation during formation of a pyroxenite vein component). This sample is therefore excluded from the dataset, inasmuch as it does not reflect the PGE abundances of a typical mantle residue. Our results show that total PGE contents for the peridotites are between 17 and 38 ppb, lying typically within the range measured for many other mantle representatives. Rhenium and Pd concentrations for the samples are significantly high compared with those of primitive mantle, whereas Os, Ir, Ru, and Pt concentrations are similar to, or slightly lower than, those of primitive mantle. The Os concentrations vary from 1.45 to 4.83 ng/g, Ir from 1.02 to 4.75 ng/g, Ru from 1.74 to 2.81 ng/g, Pt from 3.53 to 11.32 ng/g, and Pd from 4.32 to 10.64 ng/g (Table 2). As shown in Figure 6, PGEs that are characterized by remarkably different crystal chemical properties and geochemical behavior (e.g., Pd-Ir, Ru-Ir, and Pt-Ir) correlate positively, suggesting that most of the PGEs strongly partition into the same discrete phases, probably Cu-Fe-Ni sulfides. Deviations from these correlations for some samples, however, denote specific enhancements of Pd and depletions of Os relative to Ir (Fig. 6).

Chondrite-normalized PGE patterns of the peridotites, plotted in order of decreasing melting points

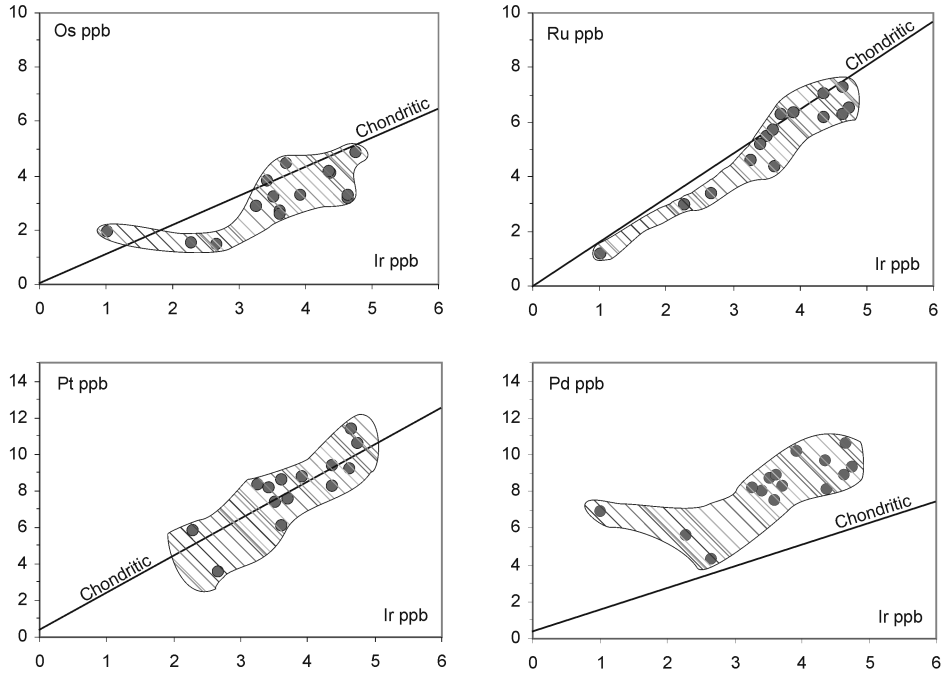

FIG. 6. Covariation of the concentrations (in ppb) of Os, Ru, Pt and Pd with Ir for the peridotites from the Northwest Anatolian ophiolites. Solid lines denote the chondritic (CI) ratios.

of the metals, demonstrate that the rocks exhibit systematics in inter-element variations (Fig. 7A). The samples are, in general, characterized by absolute PGE concentrations of 0.002–0.02 × CI-chondrite and have supra-chondritic Rh/Ir, Pd/Ir, and Pd/Pt, but near-chondritic Ru/Ir and Pt/Ir ratios. Rh/Ir and Pd/Ir ratios are significantly high at ~2.0 and 1.5 × CI-chondritic values respectively (Fig. 7B). Palladium and Rh are also significantly enriched compared with Ru. Such non-chondritic ratios and perturbations in PGE systematics are the result of strong enrichment in the light PGE (Rh and Pd) abundances relative to all other noble metals, and may be interpreted to result from recent, shallow-level petrogenetic processes. A moderate Os depletion for almost the entire suite is marked by subchondritic ratios of Os_N/Ir_N that range from 0.50 to 1.10, but remain mostly smaller than 0.80 (Table 2; Fig. 7B). This marked fractionation of Os from Ir is an unusual characteristic for melt-depleted residues and can be explained by mantle processes, which can dissolve some residual sulfides and hence lower Os (e.g., Lorand et al., 2003; Luguet et al., 2003).

P-PGE (Pt and Pd) abundances of the peridotites are highly variable. Platinum concentrations range from compositions similar to those of undepleted fertile upper mantle (~0.01 × chondritic) down to very low values (~0.003 × chondritic) that may characterize residues of high degrees of mantle melting. Palladium concentrations are also variable, and show the least degree of correlation with Ir (Fig. 6). Although no clear systematics are evident, both Pt and Pd are most depleted in samples with the lowest Al_2O_3, consistent with their origin via the highest degree of melting. This indicates that progressive melt extraction from the mantle may have some significance for mantle PGE systematics. Almost all samples display strong Pd enrichments relative to Pt (Pd_N/Pt_N = 1.6–2.2).

Petrogenetic Considerations

PGE behavior during mantle melting

The Northwest Anatolian peridotites display a remarkably variable range of degree of melt extraction as evidenced from their considerably variable Al_2O_3 and CaO abundances that range from 0.98 to

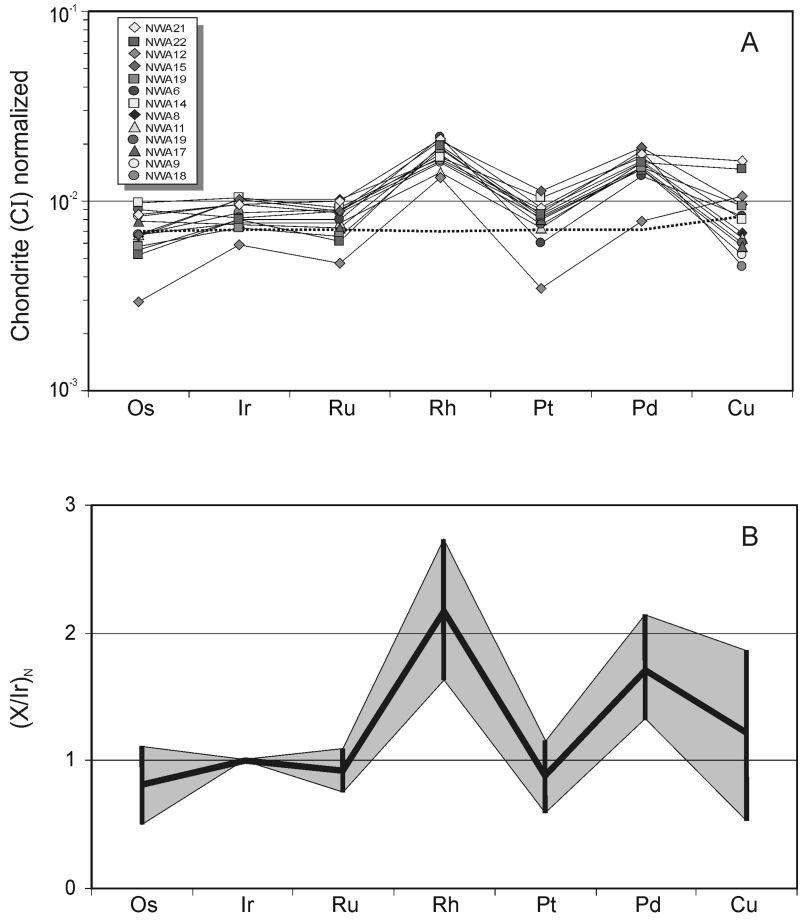

FIG. 7. A. Chondrite-normalized PGE patterns for the peridotites from Northwest Anatolian ophiolites. Also plotted for comparison are the PGE concentrations of primitive mantle (shown as a dashed line). Normalizing values and PM concentrations are from McDonough and Sun (1995). B. Average PGE concentrations normalized to Ir and CI-chondrite. The heavy line corresponds to the normalized average values.

3.37 and from 0.42 to 3.01 wt% respectively (Table 1); they provide an opportunity to investigate PGE behavior during partial melting in the mantle. Fractionated relative abundances of PGEs can be generated during partial melting of mantle peridotites, inasmuch as Ir and Os, with their greater bulk partition coefficients, are the most compatible during mantle melting, and the PGEs showing decreasing compatibility to Pd (Barnes et al., 1985; Brenan et al., 2003; Righter et al., 2004). The presence of sulfide phases during different stages of mantle melting also has a significant influence on PGE abundances of mantle residues. Processes involving varying degrees of sulfide removal or incorporation have been suggested to account for the wide variation in relative PGE abundances of both melt and residual products of mantle melting (Handler and Bennett, 1999; Rehkämper et al., 1999; Bennett et al., 2000; Bockrath et al., 2004).

Figure 8 shows the PGE abundances for the mantle peridotites plotted against Al_2O_3, as a measure of degree of melt extraction. Also plotted for comparison are the theoretical melt depletion trends calculated using a model of non-modal fractional melting. In the model calculations, the variations in PGE abundances with degree of melt depletion have been compared to melt extraction model predictions

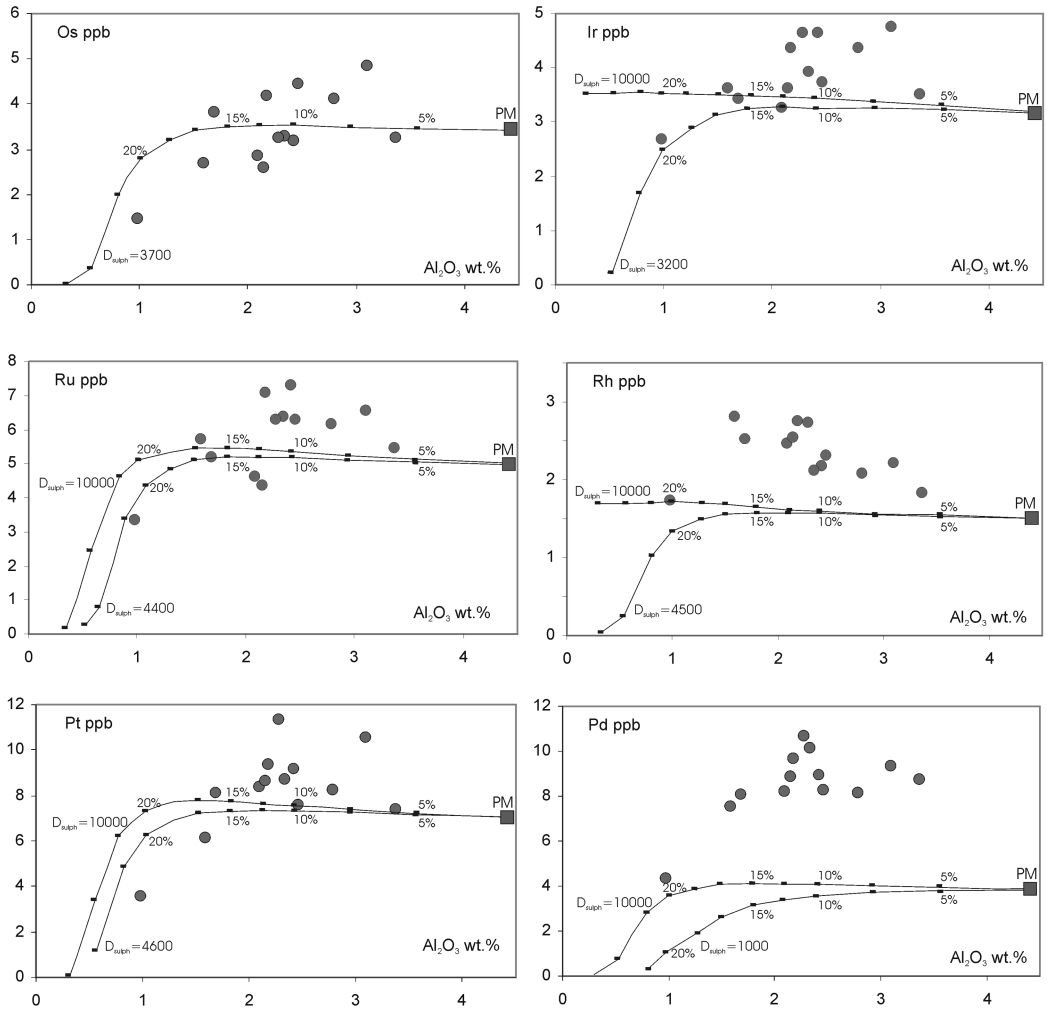

FIG. 8. Variation of Os, Ir, Ru, Rh, Pt, and Pd with Al_2O_3 for peridotites from Northwest Anatolian ophiolites. Curves model the expected variation of noble metals within a mantle residue experiencing progressive melt extraction. Calculations are non-modal incremental batch melting using a primitive upper mantle source containing 200–250 ppm S (McDonough and Sun, 1995; Holzheid and Grove, 2002) and a modal sulfide abundance of <0.1%. It is assumed that all sulfide in the source mantle will be exhausted after ~20% partial melting and that the extracted melt has an S capacity of 1000 ppm. Sulfide/melt partition coefficients ($^{PGE}D_{sulfide/melt}$) used for the modeling are from the compilation of Fleet et al. (1996), Handler and Bennett (1999), Lorand et al. (1999), Rehkämper et al. (1999), and Pearson et al. (2004). Thick marks on melt extraction curves indicate melting increments in percent.

based on PGE control by sulfides, provided that the sulfides are the major constituents for PGEs. The results of modeling indicate that variations in some of the PGE abundances (Os, Ru, Pt) of Northwest Anatolian peridotites broadly correlate with theoretical melting trends drawn for residues of mantle melting with initial composition similar to that of fertile undepleted upper mantle. A notable discrepancy between the peridotite data and the model predictions, however, is that some of the samples have PGE contents significantly greater than that which could be produced by single-stage melting and instantaneous melt extraction from a given mantle source.

There is little correlation between abundances of Ir and Al_2O_3 for the NW Anatolian peridotites, indicating the compatible behavior of Ir (e.g. $^{residual/melt}D_{Ir} > 1$). A number of samples have Ir abundances in the range of values expected for the residues of variable degree of mantle melting, but most samples display a correlation of decreasing Ir with decreasing Al_2O_3, opposite the trend expected for a suite of residues from melt extraction. Some of the samples also show considerable enrichment in Ir concentrations when compared to modeled trends of melt extraction. The lack of correlation between Ir and major element melt depletion indices is rather similar to that exhibited by many other peridotite suites, and is usually attributed to the wide variations in the range of partitioning between sulfides and basaltic silicate melt ($^{sulfide/melt}D_{Ir} \sim 10^3$–$10^5$; Bezmen et al., 1994; Fleet et al., 1996; Pearson et al., 2004). The PGE fractionation patterns for the Northwest Anatolian peridotites display an apparent coherency of the Os, Ir, and Ru relationships, indicating that these elements are mainly controlled by the same phase. The Ru/Ir ratio for almost all samples remains mostly constant over a significant range of melt extraction, implying that a phase retaining these elements was stabilized during the melting processes. The relative depletion in Os compared to Ir throughout melt extraction, however, may be explained by dissolution of some residual sulfides via melt percolation through peridotites.

Unlike all other PGEs, abundances of Rh display a negative correlation with Al_2O_3, which is consistent with the theoretical melt depletion trend of model calculations. The samples as a whole, however, display a marked displacement from the melting trend toward higher Rh concentrations, and the rate of displacement increase with increasing degree of melt extraction. This observed negative correlation, along with the elevated abundances of Rh in almost all peridotite samples relative to residues of primitive mantle estimates, can most likely be explained by the strongly compatible behavior of Rh during melt extraction, with partial control by sulfides or partitioning strongly into a major mantle phase (e.g. $^{spinel/melt}D_{Rh} \sim 41$-530; Righter et al., 2004).

Despite some scatter, which possibly reflects metasomatic introduction of sulfide and silicate phases, varying degrees of correlation between some of the PGEs and major elements are present in the peridotites from Northwest Anatolia. Positive correlations of Ru and Pt abundances with Al_2O_3, at especially moderate to high degrees of melting, may be indicative of incompatible behavior of these elements. Although some of the samples show evidence for systematic enrichment in Pt abundances, the concentration of both elements can be broadly modeled by complete control of Ru and Pt by sulfide phases during melt extraction using the range of experimentally determined sulfide/melt partition coefficient values (Fig. 8).

Pd values and Pd_N/Ir_N ratios for the peridotite samples are also broadly correlated with major-element depletion trends (Figs. 8 and 9); the most depleted peridotites with the lowest CaO (or Al_2O_3) contents, and highest Mg# have the lowest Pd concentrations and Pd_N/Ir_N ratios. Similar characteristics are also reported for many other peridotite suites worldwide (both xenolithic and orogenic; e.g. Rehkämper et al., 1997, 1999; Lorand et al., 1999; 2000) and are usually interpreted to have resulted from progressive melt extraction which fractionates less compatible P-PGEs from I-PGEs. It is, however, notable that almost all samples from the Northwest Anatolian ophiolites show evidence for a systematic enrichment in Pd_N/Ir_N ratios with respect to the range of values expected for residues of moderate degrees of partial melting from a mantle source similar in composition to the primitive upper mantle.

Increase in Pd/Ir ratios is correlated with Pd abundances, suggesting that the relatively high Pd/Ir and Rh/Ir ratios of the peridotites are most likely related to enrichment of Pd and Rh and not to the depletion of the other PGEs. This is further evidenced by the observation that the samples display average Ir, Pt, and Ru concentrations of 0.0041–0.0099 × C1-chondritic values, consistent with estimates of PGE abundances in the Earth's upper mantle (e.g. McDonough and Sun, 1995), while displaying substantially higher and more variable concentrations of Pd and Rh (0.0102–0.0211 × CI-chondrite). These characteristics, along with elevated abundances of certain incompatible lithophile elements (e.g. Ba, Th, LREE), suggest that the peridoties are not simply residues of partial melting, but also display petrological and geochemical evidence for secondary processes, the most probable of which would be melt/rock reaction that would result in refertilization of the mantle residue by basaltic melts, crystallization of silicate and sulfide phases from percolating magmas, and significant alteration in both lithophile and siderophile element abundances.

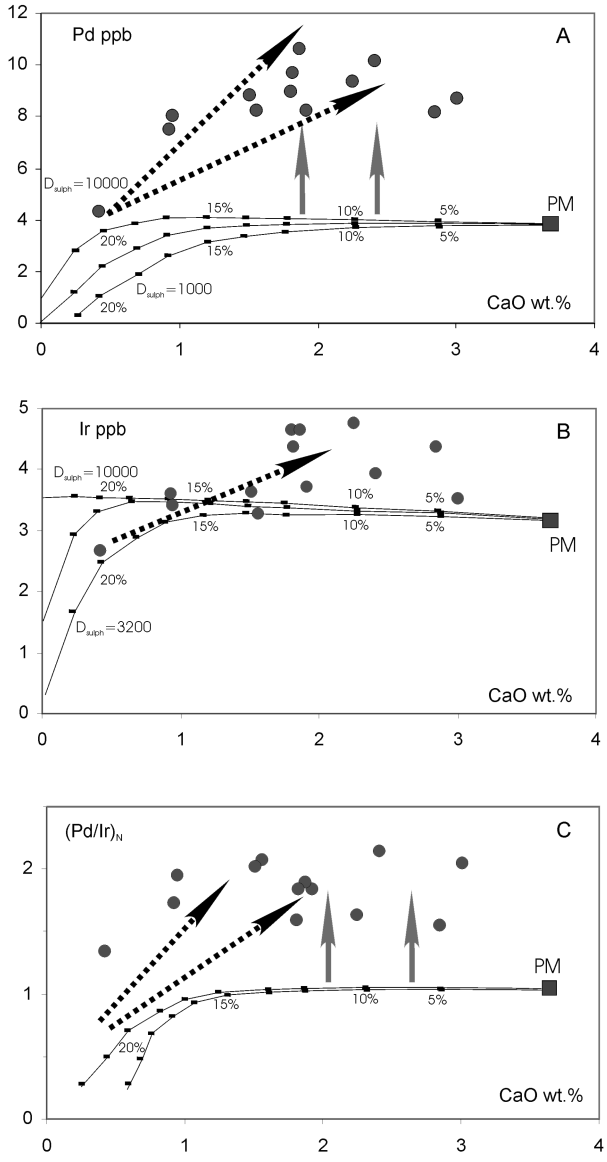

FIG. 9. Correlation of $(Pd/Ir)_N$, Pd, and Ir versus CaO (wt%) for the peridotites from Northwest Anatolian ophiolites. Modeling curves illustrate the effect of the extraction of varying degrees of partial melt (in 5% increments of melt fraction) from a fertile peridotite with ~3–4% CaO, a chondritic Pd/Ir ratio, and absolute PGE abundances similar to primitive upper-mantle estimates (3.2 ± 0.8 ppb Ir, 3.9 ± 1.0 ppb Pd; McDonough and Sun, 1995). Melting is assumed to initiate from a mantle source containing sulfide phases, but after about 20% melting (~1.0% CaO) low-melting-point sulfides are totally consumed. Modeling parameters are the same as in Figure 8. High Pd/Ir ratios and Pd concentrations for the peridotites can be explained either by the addition of sulfides to variably depleted residues (shown by grey arrows) or by sulfide addition associated with refertilization of highly depleted residues by basaltic melts (shown by dark hatched arrows).

The effect of metasomatism by percolating melts and subduction-related fluids

Numerous geochemical studies have revealed that mantle lithosphere above subduction zones has undergone some degree of chemical modification (metasomatism) that post-dates the original melting process (e.g., Pearce et al., 1999). In this context, many consider that the mantle representatives from these settings are not simply residues of basaltic melt extraction, but rather display petrographic and geochemical evidence of compositional modification either by crystallization of silicate minerals from percolating melts or by interaction between complementary liquid and solid products of mantle melting. An assessment of the impact of metasomatic processes on the bulk-rock chemistry of samples considered in this study is required to evaluate the degree to which they retain their original chemical signature as residues.

Elements that are highly incompatible are most compromised by metasomatic processes over long periods of evolution of the mantle lithosphere. Although the residence of some highly incompatible elements (bulk $D < 0.01$) is dominated by minor phases and grain boundary phenomena, a great number of incompatible elements can still be used to constrain a possible multi-process history of the upper mantle. In this study we used elements that have bulk $D_{residue/liquid}$ between 1 and 0.001 and are likely to be less affected by chemical modifications resulting from serpentinization and subsequent alteration. As is demonstrated in Figure 3, Northwest Anatolian peridotites show a range of primitive upper mantle–normalized trace element patterns. Among these, the LREE-depleted examples show smoothly increasing concentrations from left to right in the diagram, as incompatibility of the elements decreases. This indicates that the depleted mantle has lost its incompatible elements, as well as its LREE, in the order of increasing incompatibility, which can readily be explained by progressive extraction of basaltic melt from the mantle. Increases in Rb and Ba in these samples may be a result of incipient metasomatism. The majority of the samples, however, display multi-element patterns that are characterized by enrichment in highly incompatible elements. Mantle rocks that have interacted with a silicate melt would be expected to show increases in all incompatible elements, although the effects on elements such as Rb, Ba, and Nb, which are likely to have been depleted by previous melt extraction events, may not be as obvious as in the LREE. Samples that have been fluxed by subduction-derived fluids, on the other hand, would be expected to show strong enrichment in fluid-soluble large cations. Such samples tend to have negative anomalies at Ta, Nb, Zr, and Hf relative to adjacent elements on a multi-element diagram, and strong enrichment in Rb, Sr, and Ba.

Enrichment by subduction-related hydrous fluids can be anticipated in areas of supra-subduction zone lithosphere. Hydrous fluids do not usually carry LREE to any great extent, and interaction of such fluids with mantle rocks should not cause significant changes in REE concentrations. Incompatible trace element consequences of hydration of the lithosphere therefore include significant increase in highly soluble large-ion-lithophile elements (Rb, Sr, Ba, K) at the expense of insoluble high-field-strength elements (Ta, Nb, Zr, Hf). This type of enrichment is observed in most of the peridotite samples from the Northwest Anatolian suite, implying that the rocks have been affected to some extent by fluid metasomatism.

Much of the enrichment in the Northwest Anatolian peridotites, however, is related to passage of the silicate melts through lithospheric channels. Mechanisms of enrichment by the passage of silicate melts through the mantle, such as reactive porous flow or chromatographic fractionation, have been studied in detail by a number of authors (e.g., Kelemen et al., 1992, 1997) and this type of metasomatic scheme is commonly suggested to have been accompanied by enrichments in LREE, as well as other highly incompatible elements (e.g., Th, U, Ba). Modal metasomatism, which results in the formation of olivine-rich mantle representatives, is also considered to be a consequence of reaction between silicate melt and the source mantle rocks (e.g., Kelemen et al., 1997; Takazawa et al., 2003). The LREE-enriched patterns (Figs. 3 and 4) and high modal abundances of olivine in the mantle peridotites of this study can therefore be inferred to have resulted from extensive melt/solid interaction that preferentially dissolved pyroxenes and precipitated olivine.

The effects of mantle metasomatism by percolating melts can also be traced using the relative abundances of PGEs, because such processes have the potential to modify the original PGE patterns of mantle residues significantly—i.e. the chondrite-normalized PGE abundances of mantle melts increase in the order of their incompatibility from Ir

to Pd (e.g., Barnes et al., 1985). High Pd/Ir ratios of many refractory peridotite suites, for instance, are explained in terms of the introduction of metasomatic sulfides that are inferred to have been largely segregated from percolating magmas (e.g., Lorand, 1988). We therefore have attempted a semi-quantitative model to place constraints on PGE behavior during various petrogenetic processes, including: (1) simple *in situ* mantle melting and instantaneous melt extraction; (2) refertilization of a depleted mantle source by basaltic magmas; and (3) addition of sulfides, which are segregated from basaltic melts, to the source mantle. For the calculations, we used the fractional melting approach described above, but a small amount of melt retention (0.1%) is assumed here to modify and enrich the local mantle source, prior to each step of melt generation. The results are shown in Figure 9, where we compare the observed compositions of the peridotite samples with the theoretical fractional melting trends for melting of a simplified two system comprising sulfides and mantle silicates.

The calculated melting trends suggest that a simple melting and melt extraction process should be associated with increasing Ir, because this element is considered to be compatible during the entire melting process ($^{sulfide/melt}D_{Ir} \sim 10^5$; Pearson et al., 2004). Because of its high sulfide/melt distribution coefficient ($^{sulfide/melt}D_{Pd} \sim 10^4$; Lorand et al., 1999; Rehkämper et al., 1999) Pd is also inferred to behave similarly in the presence of sulfide phases—i.e. at low to moderate degrees of partial melting (F <15%). Following the total consumption of the sulfides at greater degrees of partial melting (e.g., F >20%; ~1.0% CaO), however, Pd behaves incompatibly because partitioning of this element between primary mantle phases and silicate melt is fairly low ($^{olivine/melt}D_{Pd}$ 0.0075–0.21; Brenan et al., 2003; Righter et al., 2004). Further melting would therefore result in a sharp decrease both in Pd abundance and in the Pd/Ir ratio along the melting trends.

The theoretical melting trajectories in Figure 9 clearly demonstrate that a single-stage melting and instantaneous melt extraction from a mantle source similar in composition to the primitive upper mantle cannot account for the high absolute Pd and Ir concentrations and high Pd_N/Ir_N ratios of the Northwest Anatolian peridotites. One possible option to explain strong Pd and Ir enrichments associated with continuous mantle melting is that melt depletion was accompanied by addition of sulfides to the solid residue. This process would increase Pd abundances of the melting residues without affecting the lithophile-element concentrations significantly, leading to the vertical melting trends obtained in Figure 9. It is notable, however, that the enrichment of Pd in the Northwest Anatolian peridotites is accompanied by an increase in CaO contents of the rocks (for moderate-degree melting residues in particular; F >10), suggesting that the relative distributions of PGEs cannot be explained solely by sulfide addition to variably depleted residues.

A proposal that the relative enrichment in Pd concentrations is a result of interaction between depleted solid mantle and segregated melts would provide a much more satisfactory explanation. Such a refertilization process would re-enrich the local mantle region in basaltic components (and in incompatible lithophile elements) and cause an increase in Pd concentrations and Pd/Ir ratios that would result from the addition of sulfides segregated from mantle-derived melts. The effect of the addition of sulfides originated from mantle-derived basaltic magmas on variably depleted solid residues is shown in Figure 9, where some fraction of sulfide liquid is assumed to be segregated by the melt during passage through the solid mantle residue; the plots show that various aspects of the PGE geochemistry of the Northwest Anatolian peridotites are likely attributable to metasomatic effects that involve the introduction of sulfides, probably accompanied by silicate melts. Modeling of melt re-enrichment involving the addition of new sulfides to variably depleted mantle residues during magma/mantle interaction produces elevation of the Pd_N/Ir_N ratio to supra-chondritic levels and the elevated P-PGE contents. These characteristics are explained in terms of melt + sulfide addition where Ca (and also Al) is introduced by the melt and Pd is introduced by additional sulfide. Melt introduction may also be responsible for the widely varying non-chondritic Ca/Al ratios and incompatible-lithophile-element–enriched nature of the peridotites.

Peridotites from Northwest Anatolia are also characterized by their distinct depletion in Pt compared with the other P-PGE elements of Pd and Rh (Fig. 7). The discrete behavior of Pt relative to the other PGEs is also documented in many other massif peridotite and xenolith suites and is usually attributed to the occurrence of Pt-rich sulfide phases, potentially fractionating Pt from other P-PGE (e.g., Handler and Bennett, 1999). Recent studies further suggest that PGEs least soluble in silicate melts (e.g., Os, Ir, Ru, Pt) may precipitate as

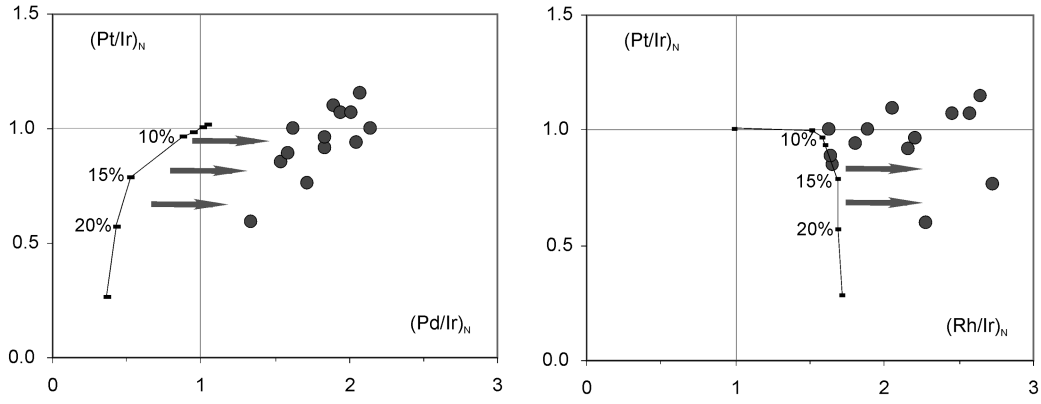

FIG. 10. Models of Pt_N/Ir_N, Rh/Ir, and Pd_N/Ir_N in Northwest Anatolian ophiolites based on mass balance equations for incremental batch melting of the sulfide phase, assuming all PGEs reside in the base-metal sulfides. Curves denote the PGE fractionation trends by partial melting; arrows indicate the effects of addition of sulfides segregated from mantle melts to a depleted mantle. Normalizing values are from McDonough and Sun (1995). The mantle source and the modeling parameters are the same as in Figure 8.

discrete refractory alloys (e.g., Bockrath, et al., 2004). As a result, compared to the other P-PGEs, Pt is not as effectively mobilized during melting and melt migration through residual mantle, lowering Ir/Pd and Pt/Pd ratios of the melt. This is also evident from theoretical modeling by Rehkämper et al. (1999), who demonstrated that mantle melting characteristically produces melts with $Pt_N/Ir_N < Pd_N/Ir_N$. Addition of sulfides segregated from such melts to a depleted mantle produces peridotites with near-chondritic Pt_N/Ir_N, but significantly high Pd_N/Ir_N (Fig. 10). Thus, shallow-level petrogenetic processes including simple refertilization by silicate melts and addition of sulfides to the depleted mantle residues can account for the discrepancy between the near-chondritic Ru/Ir and Pt/Ir ratios and the supra-chondritic Pd/Ir, Rh/Ir and Pd/Pt ratios observed in the Northwest Anatolian peridotites.

Discussion: PGE and Chromium Enrichment in Mantle Rocks

A significant number of recent studies have revealed the importance of mantle sulfides concerning the distributions and relative abundances of PGEs in mantle rocks (e.g., Rehkämper et al., 1999; Alard et al., 2000; Bockrath et al., 2004). As is often pointed out, base-metal sulfides are the major hosts of PGEs in fertile mantle rocks (e.g. Mitchell and Keays, 1981), and in many cases this is evidenced by strong positive correlations between whole-rock PGE contents, Cu, Ni, and S (Lorand et al., 1999). Experiments and observations indicate that monosulfide solid solutions (MSS) preferentially accommodate refractory PGE (Os, Ir, Ru,) during melting, relative to Cu-rich sulfides, which concentrate Pd and Re (Lorand and Alard, 2001; Pearson et al., 1998, 2004). For low to moderate degrees of melting (<15%), residual sulfides can be shown to buffer PGE abundances in mantle peridotites to relatively constant levels because of the high sulfide/melt partition coefficients for these elements (e.g. $^{sulfide/melt}D = \sim 10^5\,[Ir] - 10^4\,[Pd]$; Lorand et al., 1999; Pearson et al., 2004). At high degrees of melting (>20%), low-melting-point sulfides are likely to be consumed (Fig. 8). Palladium-group PGEs partition preferentially into the melt phase during high degrees of melting, due mainly to the breakdown of the sulfide phases and dissolution during decompression. In contrast, the higher melting point siderophile elements (I-PGE) remain in the residue, and may be stabilized in either alloy phases or high-melting-point residual Ru-Os-Ir sulfides (Brenan and Andrews, 2001; Bockrath et al., 2004). Processes of mantle melting in this manner would therefore be expected to produce highly P-PGE–depleted residues with highly fractionated chondrite-normalized PGE pattern and oversaturated basaltic melts with respect to the least-soluble refractory PGEs.

The relative abundances of PGE systematics and chondrite-normalized distribution patterns show

that the Northwest Anatolian peridotites are characterized by supra-chondritic Pd_N/Ir_N and Rh_N/Ir_N ratios, a feature that is complementary to the trends expected to be produced by *in situ* melting preferentially consuming the lower-melting-point sulfides. Similar PGE fractionations characterized by high ratios of P-PGE over I-PGE are generally interpreted to be an intrinsic source feature common to many continental lithospheric mantle samples (e.g., Pattou et al., 1996; Lorand et al., 1999). However, the strong correlations of the Pd_N/Ir_N and Rh_N/Ir_N ratios with melt depletion indices of major oxides, especially at low to moderate degrees of melting, suggest that such enrichment in P-PGEs is not a source characteristic, but can most likely be interpreted in terms of sulfide addition by sulfur-saturated melts (e.g. Rehkämper et al., 1999; Pearson et al., 2004). Alard et al. (2000) also postulated that pentlandite-dominated interstitial sulfides, the products of the crystallization of sulfide-bearing metasomatic fluids, exhibit low Os and Ir abundances but high Pd/Ir ratios. In contrast, the silicate-enclosed sulfides (including MSS), which are produced as the residues of melting processes, are characterized by high Ir and Os abundances and low Pd/Ir ratios. The non-chondritic siderophile-element patterns and particularly high Pd and Rh (relative to Os and Ir) abundances of the Northwest Anatolian periotites can thus most likely be explained by addition of interstitial sulfides originating from solid/melt reactions, following moderate degrees of melting and melt extraction from the mantle. This is further evidenced by relative depletions in Pt and supra-chondritic ratios of Pd_N/Pt_N, as the marked fractionation of Pt from Pd can most likely be explained as originating from interstitial sulfides (e.g., pentlandite) that accommodate a substantial amount of Pd and Rh (up to a few percent), but only trace amounts of Pt (e.g., Ballhaus and Ryan, 1995; Alard et al., 2000; Ballhaus and Sylvester, 2000).

It is generally assumed that PGEs and chromium behave compatibly during dry partial melting of the upper mantle (e.g., Mitchell and Keays, 1981; Dick and Bullen, 1984), and these metals therefore show restricted mobility at mid-ocean ridges (i.e., no chromitite deposits have yet been observed in abyssal peridotites). In contrast, mantle fluxing by hydrous fluids and melts is a typical feature of SSZ environments. In these environments, mantle peridotites can be melted to a higher degree than beneath oceanic ridges and mid-plate settings, because the mantle wedge is fluxed by fluids released from the subducting oceanic lithosphere (e.g., Pearce, et al., 1984). A number of recent studies also have emphasized the importance of water-saturated melting on the behavior and relative distribution of PGEs (and Cr) during the interaction among fluids, silicate melts, and the residual upper mantle rocks in subduction-zone settings.

The relative enrichment of PGEs and chromium in the residual products of the upper mantle is, in many cases, ascribed to element mobilization. The chromitite deposits in Northwest Anatolian ophiolites, as well as many other deposits worldwide, are commonly enclosed in dunite envelopes surrounded by moderately depleted harzburgites (Lago et al., 1982; Roberts, 1988; Zhou et al., 1996, 1998; Melcher et al., 1997). We interpret the dunites of this type within the Northwest Anatolian ophiolites as originating from melt percolation and not by partial melting, because the degree of depletion required to produce the dunite compositions by instantaneous melting and melt extraction is not reflected by the degree of melt extraction observed in the residual products. Results of theoretical modeling show that the majority of the peridotites from northwest Anatolia are solid residues formed after a moderate degree of mantle melting, and yet the samples contain modal olivine that is significantly higher than that would be expected for residues of a moderate degree of partial melting. This characteristic is likely to have resulted from melt/solid reaction that preferentially dissolves clinopyroxene and incongruently melts orthopyroxene, and precipitates olivine from the melt (e.g., Kelemen et al., 1992). Similar occurrences of reactive dunite and harzburgite bodies found in many Alpine-type ophiolites are also interpreted as the products of magma reacting with surrounding lherzolites (Büchl et al., 2004; Grieco et al., 2004). In this context, the reaction is suggested to have taken place by a mechanism in which the melt, originally in equilibrium with a mantle mineral assemblage at depth, is saturated only in olivine upon upwelling. The melt thus reacts with clinopyroxene and orthopyroxene of the lherzolite to precipitate olivine. The dissolution of pyroxenes will continue until chemical equilibrium between melt and the surrounding lherzolite is achieved and such reaction derives olivine-saturated melts into the chromite stability field, leading to the formation of extensive chromite deposits.

Experimental studies of Matveev and Ballhaus (2002) on water-oversaturated basalts further

demonstrate that ophiolitic chromite deposits would form only where primitive melts are present, saturated in olivine-chromite and rich in water. Such conditions most likely occur in supra-subduction zone environments because this is the only tectonic setting that might generate primitive melts with primary water contents sufficient to exsolve a fluid phase necessary for chromite formation. Thus, the chromite-bearing reactive harzburgite and dunite bodies within the Northwest Anatolian ophiolites can be interpreted to be the result of chromite-forming, olivine-dissolving melt/rock reactions produced when subduction-related basaltic melts migrated by porous flow through peridotite channels and mixed with oxidized, volatile-rich melts in the supra-subduction mantle (e.g., Ohara et al., 2002). Hence, the formation of the primary igneous chromite in the Northwest Anatolian ophiolites can be explained as crystallizing from water-oversaturated melts (with subduction-related geochemical signatures) in the supra-subduction zone mantle.

The PGE patterns of the peridotites determined in this study are similar to those observed in many other chromite-bearing ophiolite complexes (e.g., McElduff and Stumpfl, 1990; Prichard and Lord, 1990; Melcher et al., 1997; Zhou et al., 1998). The depletion of Pt relative to Ir, Os, and Ru is also a common characteristic observed in the vast majority of ophiolites worldwide. This suggests that ophiolite complexes containing large podiform chromite deposits concentrate PGEs by similar petrogenetic processes.

Concluding Remarks

The Northwest Anatolian ophiolite complex contains mantle peridotites that represent a fragment of oceanic lithosphere formed and subsequently modified in a supra-subduction zone environment. The peridotites are mainly clinopyroxene-poor spinel-harzburgites and dunites with subordinate lherzolites (e.g., 0.18–2.37 wt.% Al_2O_3), which, in terms of major-element chemistry, strongly resemble peridotites originated as the solid residues of 5–20% partial melting. Lithophile trace-element variations of the rocks, however, indicate that the peridotites bear evidence of impregnation by instantaneous melt fractions enriched in incompatible elements. The composition of harzburgites and dunites in Northwest Anatolian ophiolites are consistent with an origin through interaction between melt-depleted residue and incompatible element–enriched basaltic magma. Lherzolites in this suite represent the residuum of an earlier episode of depletion by partial melting and melt extraction. During formation of chromium deposits, a large volume of magma passed through, and reacted with, the lherzolite. Such melt/rock reaction would have further depleted the lherzolite in modal pyroxene to form the harzburgite and dunite, both of which would have been enriched in certain incompatible elements, resulting in enrichment of some strongly incompatible elements (e.g. Ba, U, LREE).

The samples, as a whole, have fractionated chondrite-normalized PGE patterns that are characterized by supra-chondritic ratios of Rh_N/Ir_N, Pd_N/Ir_N, Pd_N/Pt_N, and Ir_N/Os_N. Theoretical models of melt extraction indicate that these characteristics cannot be reconciled with a simple *in situ* melt extraction and removal of sulfide phases, but most likely reflect a multi-stage petrogenetic process that selectively enriched the local mantle environment in incompatible and less refractory siderophile elements that are mobilized by silicate melts (or fluids) during continuous melt percolation. The movement of the metasomatic sulfide phases that are likely to have existed in the upper mantle has the potential to produce supra-chondritic Pd/Ir and Rh/Ir ratios in the mantle section of the oceanic lithosphere. The results of quantitative model calculations indicate that the addition of sulfides originating from interaction between solid mantle and percolating hydrous basaltic melts may account for the strongly supra-chondritic ratios of both Pd/Ir and Ir/Os, as well as for the formation of abundant chromite deposits within the ophiolite complex. We thus envisage that the non-chondritic relative abundances of highly siderophile elements found in various mantle samples from the Northwest Anatolian ophiolite complex are due to sulfide differentiation within the mantle, by partial melting, and melt + sulfide addition through melt/solid interaction. Many aspects of the PGE systematics of the Northwest Anatolian peridotites can thus be attributed to metasomatic processes that involve the introduction of sulfide along with silicate melt.

Acknowledgments

This study was funded by TUBITAK through a research project grant (104Y171). We thank Aykut Guctekin and Daghan Celebi for their help with the sample preparation.

REFERENCES

Alard, O., Griffin, W. L., Lorand, J. P., Jackson, S. E., and O'Reilly, S. Y., 2000, Non-chondritic distribution of the highly siderophile elements in mantle sulfides: Nature, v. 407, p. 891–894.

Anders, E., and Grevesse, N., 1989, Abundances of the elements: Meteoritic and solar: Geochimica et Cosmochimica Acta, v. 53, p. 197–214.

Ballhaus, C., 1998, Origin of podiform chromite deposits by magma mingling: Earth and Planetary Science Letters, v. 156, p. 185–193.

Ballhaus, C., and Ryan, C. G., 1995, Platinum group elements in Merensky Reef. 1. PGE in solid solution in base metal sulfides and the down-temperature equilibration history of Merensky ores: Contributions to Mineralogy and Petrology, v. 122, p. 241–251.

Ballhaus, C., and Sylvester, P., 2000, Noble metal enrichment processes in the Merensky Reef, Bushveld complex: Journal of Petrology, v. 41, p. 545–561.

Barnes, S.-J., Naldrett, A. J., and Gorton, M. P., 1985, The origin of the fractionation of platinum-group elements in terrestrial magmas: Chemical Geology, v. 53, p. 303–323.

Beccaletto, L., and Jenny, C., 2004, Geology and correlation of the Ezine zone: A Rhodope fragment in NW Turkey: Turkish Journal of Earth Sciences, v. 13, p. 145–176.

Bennett, V. C., Norman, M. D., and Garcia, M. O., 2000, Rhenium and platinum group element abundances correlated with mantle source components in Hawaiian picrites: Sulphides in the plume: Earth and Planetary Science Letters, v. 183, p. 513–526.

Bezmen, N. I., Asif, M., Brugmann, G. E., Romanenko, I. M., and Naldrett, A. J., 1994, Distribution of Pd, Ru, Rh, Ir, Os, and Au between sulfide and silicate melts: Geochimica et Cosmochimica Acta, v. 58, p. 1251–1260.

Bockrath, C., Ballhaus, C., and Holzheid, A., 2004, Fractionation of the platinum-group elements during mantle melting: Science, v. 305, p. 1951–1953.

Bonatti, E., and Michael, P. J., 1989, Mantle peridotites from continental rifts to ocean basins to subduction zones: Earth and Planetary Science Letters, v. 91, p. 297–311.

Brandon, A. D., Snow, J. E., Walker, R. J., Morgan, J. W., and Mock, T. D., 2000, ^{190}Pt-^{186}Os and ^{187}Re-^{187}Os systematics of abyssal peridotites: Earth and Planetary Science Letters, v. 177, p. 319–335.

Brenan, J. M., and Andrews, D., 2001, High-temperature stability of laurite and Ru-Os-Ir alloy and their role in PGE fractionation in mafic magmas: Canadian Mineralogist, v. 39, p. 341–360.

Brenan, J. M., McDonough, W. F., and Dalpe, C., 2003, Experimental constraints on the partitioning of rhenium and some platinum-group elements between olivine and silicate melt: Earth and Planetary Science Letters, v. 212, p. 135–150.

Büchl, A., Brügmann, G. E., Batanova, V. G., Münker, C., and Hofmann, A. W., 2002, Melt percolation monitored by Os isotopes and HSE abundances: A case study from the mantle section of the Troodos Ophiolite: Earth and Planetary Science Letters, v. 204, p. 385–402.

Büchl, A., Brügmann, G. E., and Batanova, V. G., 2004, Formation of podiform chromitite deposits: Implications from PGE abundances and Os isotopic compositions of chromites from the Troodos complex, Cyprus: Chemical Geology, v. 208, p. 217–232.

Dick, H. J. B., and Bullen, T., 1984, Chromian spinel as a petrogenetic indicator in abyssal and alpine-type peridotites and spatially associated lavas: Contributions to Mineralogy and Petrology, v. 86, p. 54–76.

Fleet, M. E., Crocket, J. H., and Stone, W. E., 1996, Partitioning of platinum-group elements (Os, Ir, Ru, Pt, Pd) and gold between sulfide liquid and basalt melt: Geochimica et Cosmochimica Acta, v. 60, p. 2397–2412.

Grieco, G., Ferrario, A., and Mathez, E. A., 2004, The effect of metasomatism on the Cr-PGE mineralization in the Finero Complex, Ivrea Zone, Southern Alps: Ore Geology Reviews, v. 24, p. 294–314.

Griffin, W. L., Spetsius, Z. V., Pearson, N. J., and O'Reilly, S. Y., 2002, In situ Re-Os analysis of sulfide inclusions in kimberlitic olivine: New constraints on depletion events in the Siberian lithospheric mantle: Geochemistry, Geophysics, Geosystems, v. 3 (paper no. 1069).

Ghiorso, M. S., and Sack, R. O., 1995, Chemical mass transfer in magmatic processes IV. A revised and internally consistent thermodynamic model for the interpolation and extrapolation of liquid-solid equilibria in magmatic systems at elevated temperatures and pressures: Contributions to Mineralogy and Petrology, v. 119, p. 197–212.

Handler, R. M., and Bennett, V. C., 1999, Behavior of platinum-group elements in the subcontinental mantle of eastern Australia during variable metasomatism and melt depletion: Geochimica et Cosmochimica Acta, v. 63, p. 3597–3618.

Hellebrand, E., Snow, J. E., Dick, H. J. B., and Hoffmann, A. W., 2001, Coupled major and trace elements as indicators of extent of melting in mid-ocean-ridge peridotites: Nature, v. 410, p. 677–681.

Holzheid, A., and Grove, T. L., 2002, Sulfur saturation limits in silicate melts and their implications for core formation scenarios for terrestrial planets: American Mineralogist, v. 87, p. 227–237.

Kelemen, P. B., Dick, H. J. B., and Quick, J. E., 1992, Formation of harzburgite by pervasive melt/rock reaction: Nature, v. 358, p. 635–641.

Kelemen, P. B., Hirth, G., Shimizu, N., Spiegelman, M., and Dick, H. J. B., 1997, A review of melt migration processes in the adiabatically upwelling mantle

beneath oceanic spreading ridges: Philosophical Transactions Royal Society London, v. A 355, p. 283–318.

Kinzler, R. J., 1997, Melting of mantle peridotite at pressures approaching the spinel to garnet transition: Application to mid-ocean ridge basalt petrogenesis: Journal of Geophysical Research, v. 102, p. 853–874.

Lago, B., Rabinowicz, M., and Nicolas, A., 1982, Podiform chromite ore bodies: A genetic model: Journal of Petrology, v. 23, p. 103–125.

Lenoir, X., Garrido, C., Bodinier, J. L., and Dautria, J. M., 2000, Contrasting geochemical lithospheric mantle domains beneath Massif Central (France) revealed by peridotite xenoliths: Geodynamic heritage versus Cenozoic plume-lithosphere interaction: Earth and Planetary Science Letters, v. 181, p. 359–375.

Lorand, J. P., 1988, Fe–Ni–Cu sulfides in tectonite peridotites from the Maqsad district, Semail ophiolite, southern Oman: Implications for the origin of the sulfide component in the oceanic upper mantle: Tectonophysics, v. 151, p. 57–73.

Lorand, J. P., and Alard, O., 2001, Platinum-group element abundances in the upper mantle: New constraints from in situ and whole-rock analyses of Massif Central xenoliths (France): Geochimica et Cosmochimica Acta, v. 65, p. 2789–2806.

Lorand, J. P., Gros, M., and Pattou, L., 1999, Fractionation of platinum group element in the upper mantle: A detailed study in Pyrenean orogenic peridotites: Journal of Petrology, v. 40, p. 951–987.

Lorand, J. P., Reisberg, L., and Bedini, R. M., 2003, Platinum-group elements and melt percolation processes in Sidamo spinel peridotite xenoliths, Ethiopia, East African Rift, *in* Bennett, V., Brandon, A., Neal, M., and Horan, M., eds., Highly siderophile elements in the Earth and meteorites: A volume in honour of John Morgan: Chemical Geology, v. 196, p. 57–76.

Lorand, J. P., Schmidt, G., Palme, H., and Kratz, K. L., 2000, Highly siderophile element geochemistry of the Earth's mantle: New data for the Lanzo (Italy) and Ronda (Spain) orogenic peridotite bodies: Lithos, v. 53, p. 149–164.

Luguet, A., Alard, O., Lorand, J. P., Pearson, N. J., Ryan, C. G., and O'Reilly, S. Y., 2001, Laser-ablation microprobe (LAM)-ICPMS unravels the highly siderophile element geochemistry of the oceanic mantle: Earth and Planetary Science Letters, v. 189, p. 285–294.

Luguet, A., Lorand, J. P., and Seyler, M., 2003, Sulfide petrology and highly siderophile element geochemistry of abyssal peridotites: A coupled study of samples from the Kane fracture zone (45 degrees W, 23 degrees 20N, MARK area, Atlantic Ocean): Geochimica et Cosmochimica Acta, v. 67, p. 1553–1570.

Matveev, S., and Ballhaus, C., 2002, Role of water in the origin of podiform chromitite deposits: Earth and Planetary Science Letters, v. 203, p. 235–243.

McDonough, W. F., and Sun, S.-s., 1995, The composition of the Earth: Chemical Geology, v. 120, p. 223–253.

McElduff, B., and Stumpfl, E. F., 1990, Platinum-Group Minerals from the Troodos Ophiolite, Cyprus: Mineralogy and Petrology, v. 42, p. 211–232.

McKenzie, D. P., and O'Nions, R. K., 1991, Partial melt distribution from inversion of rare earth element concentrations: Journal of Petrology, v. 32, p. 1021–1991.

Meisel, T., Walker, R. J., Irving, A. J., and Lorand, J. P., 2001, Osmium isotopic compositions of mantle xenoliths: A global perspective: Geochimica et Cosmochimica Acta, v. 65, p. 1311–1323.

Meisel, T., Walker, R. J., and Morgan, J. W., 1996, The osmium isotopic composition of the Earth's primitive upper mantle: Nature, v. 383, p. 517–520.

Melcher, F., Grum, W., Simon, G., v. Thalhammer, T., and Stumpfl, E. F., 1997, Petrogenesis of the ophiolitic giant chromite deposits of Kempirsai, Kazakhstan: A study of solid and fluid inclusions in chromite: Journal of Petrology, v. 38, p. 1419–1458.

Mitchell, R. H., and Keays, R. R., 1981, Abundance and distribution of gold, palladium and iridium in some spinel and garnet lherzolites: Implications for the nature and origin of precious metal rich intergranular components in the upper mantle: Geochimica et Cosmochimica Acta, v. 45, p. 2425–2445.

Morgan, J. W., Walker, R. J., Brandon, A. D., and Horan, M., 2001, Siderophile elements in Earth's upper mantle and lunar breccias: Data synthesis suggest manifestations of the same late influx: Meteoritics and Planetetary Science, v. 36, p. 1257–1275.

Ohara, Y., Stern, R. J., Ishii, T., Yurimoto, H., and Yamazaki, T., 2002, Peridotites from the Mariana Trough: First look at the mantle beneath an active back-arc basin: Contributions to Mineralogy and Petrology, v. 143, p. 1–18.

Okay, A. I., Harris, N. B. W., and Kelley, S. E., 1998, Exhumation of blueschists along a Tethyan suture in northwest Turkey: Tectonophysics, v. 285, p. 275–299.

Önen, A. P., 2003, Neotethyan ophiolitic rocks of the Anatolides of NW Turkey and comparison with Tauride ophiolites: Journal of the Geological Society, v. 160, p. 947–962.

Parkinson, I. J., and Pearce, J. A., 1998. Peridotites from the Izu-Bonin-Mariana forearc (ODP Leg 125): Evidence for mantle melting and melt-mantle interaction in a supra-subduction zone setting: Journal of Petrology, v. 39, p. 1577–1618.

Pattou, L., Lorand, J. P., and Gros, M., 1996, Non-chondritic platinum-group element ratios in the Earth's mantle: Nature, v. 379, p. 712–715.

Pearce, J. A., Barker, P. F., Edwards, S. J., Parkinson, I. J., and Leat, P. T., 1999, Geochemical and tectonic significance of peridotites from the South Sandwich arc-basin system, South Atlantic: Contributions to Mineralogy and Petrology, v. 139, p. 36–53.

Pearce, J. A., Lippard, S. J., and Roberts, S., 1984, Characteristics and tectonic significance of supra-subduction zone ophiolites, *in* Kokelaar, B. P., and Howells, M. F., eds., Marginal basin geology: Special Publication, Geological Society of London, v. 16, p. 77–94.

Pearson, D. G., Irvine, G. J., Ionov, D. A., Boyd, F. R., and Dreibus, G. E., 2004, Re-Os isotope systematics and platinum group element fractionation during mantle melt extraction: A study of massif and xenolith peridotite suites: Chemical Geology, v. 208, p. 29–59.

Pearson, D. G., Shirey, S. B., Harris, J. W., and Carlson, R. W., 1998, A Re-Os isotope study of sulfide diamond inclusions from the Koffiefontien kimberlite, S. Africa: Constraints on diamond crystallisation ages and mantle Re–Os systematics: Earth and Planetary Science Letters, v. 160, p. 311–326.

Plessen, H. G., and Erzinger, J., 1998, Determination of the platinum group elements and gold in twenty rock reference samples by inductively coupled plasma-mass spectrometry (ICP-MS) after pre-concentration by nickel sulfide fire assay: Geostandard Newsletter, v. 22, p. 187–194.

Prichard, H. M., and Lord, R. A., 1990, Platinum and palladium in the Troodos ophiolite complex, Cyprus: Canadian Mineralogy, v. 28, p. 607–617.

Puchtel, I. S., and Humayun, M., 2001, Platinum-group element fractionation in a komatiite basalt lava lake: Geochimica et Cosmochimica Acta, v. 65, p. 2979–2993.

Rehkämper, M., Halliday, A. N., Alt, J., Fitton, J. G., Zipfel, J., and Takazawa, E., 1999, Non-chondritic platinum-group element ratios in oceanic mantle lithosphere: Petrogenetic signature of melt percolation?: Earth and Planetary Science Letters, v. 172, p. 65–81.

Rehkämper, M., Halliday, A. N., Barfod, D., Fitton, G., Dawson, J. B., 1997, Platinum-group elements abundance in different mantle environments: Science, v. 278, p. 1595–1598.

Righter, K., Campbell, A. C, Humayun, M., and Hervig, R. L., 2004, Partitioning of Ru, Rh, Pd, Re, Ir, and Au between Cr-bearing spinel, olivine, pyroxene, and silicate melts: Geochimica et Cosmochimica Acta, v. 68, p. 867–880.

Roberts, S., 1988, Ophiolitic chromitite formation: A marginal basin phenomenon: Economic Geology, v. 83, p. 1034–1036.

Sengor, A. M. C., and Yilmaz, Y., 1981, Tethyan evolution of Turkey: A plate tectonic approach: Tectonophysics, v. 75, p. 181–241.

Seyfried, W. E., and Dibble W. E., Jr., 1980, Seawater–peridotite interaction at 300°C and 500 bars: Implications for the origin of oceanic serpentinites: Geochimica et Cosmochim Acta, v. 44, p. 309–322.

Shervais, J. W., 2001. Birth, death, and resurrection: The life cycle of suprasubduction zone ophiolites: Geochemistry, Geophysics, Geosystems, v. 2 (paper no: 2000GC000080).

Snow, J. E., and Schmidt, G., 1998, Constraints on Earth accretion deduced from noble metals in the oceanic mantle: Nature, v. 391, p. 166–169.

Takazawa, E., Okayasu, T., and Satoh, K., 2003, Geochemistry and origin of the basal lherzolites from the northern Oman ophiolite (northern Fizh block): Geochemistry, Geophysics, Geosystems, v. 4 (paper no. 1021).

Zhou, M.-F., Robinson, P. T., Malpas, J., and Zijin, L., 1996, Podiform chromitites in the Luobusa Ophiolite (southern Tibet): Implications for melt/rock interaction and chromite segregation in the upper mantle: Journal of Petrology, v. 37, p. 3–21.

Zhou, M.-F., Sun, M., Keays, R. R., and Kerrich, R. W., 1998, Controls of platinum-group elemental distributions of podiform chromitites: A case study of high-Cr and high-Al chromitites from Chinese orogenic belts: Geochimica et Cosmochimica Acta, v. 62, p. 677–688.

Zou, H., 1998, Trace element fractionation during modal and non-modal dynamic melting and open-system melting: A mathematical treatment: Geochimica et Cosmochimica Acta, v. 62, p. 1937–1945.